

Gas-Phase IR Spectroscopy of Nucleobases

Mattanjah S. de Vries

Abstract IR spectroscopy of nucleobases in the gas phase reflects simultaneous advances in both experimental and computational techniques. Important properties, such as excited state dynamics, depend in subtle ways on structure variations, which can be followed by their infrared signatures. Isomer specific spectroscopy is a particularly powerful tool for studying the effects of nucleobase tautomeric form and base pair hydrogen-bonding patterns.

Keywords Clusters · Gas phase · Hole burning · IR spectroscopy · Nucleobases · R2PI · REMPI

Contents

1	Introduction	272
2	Techniques	273
2.1	IR-UV Double Resonance	273
2.2	Fourier Transform Microwave Spectroscopy	273
2.3	Helium Droplets	274
2.4	Cavity Ringdown Spectroscopy and Multipass Absorption	274
3	Monomers and Tautomeric Forms	274
3.1	Purines	274
3.2	Pyrimidines	279
3.3	Excited State IR	281
3.4	Ionic Nucleobases and Nucleotides	282
4	Cluster Structures	283
4.1	Base Pairs	284
4.2	Clusters with Water	285
4.3	Stacking vs H-Bonding Structures	287

M.S. de Vries (✉)

Department of Chemistry and Biochemistry, University of California, Santa Barbara,
CA 93106, USA

e-mail: devries@chem.ucsb.edu

5	Excited State Dynamics	288
6	Summary and Outlook	291
	References	292

Abbreviations

A	Adenine
C	Cytosine
DRS	Double resonant spectroscopy
G	Guanine
T	Thymine
U	Uracil

1 Introduction

Gas-phase techniques provide a reductionist approach to the study of nucleobases and nucleotides. Collision-free conditions in vacuo provide insight into the intrinsic properties of individual molecules, free of any interactions. Without such isolation, many fundamental properties can be masked by the biological environment, such as the macromolecular structure of the double helix, base pairing interactions, and the role of the solvent. Among the properties of interest are conformational preferences, tautomeric population distributions, hydrogen bonded and pi-stacking structures, inter- and intramolecular interactions, and excited state dynamics. Once such properties are mapped out for isolated bases, one can hope to extrapolate to more complex systems, including larger DNA segments and solvent contributions. Many aspects of these properties can be probed with the help of IR spectroscopy, which is particularly diagnostic for structural variation, especially when hydrogen bonding is involved.

In order to derive structural information from infrared frequencies, input is required from quantum chemical calculations at computational levels which match the experimental resolution. Experimentally, gas-phase conditions imply extremely low sample densities, requiring special techniques in order to acquire infrared data. Some of those techniques involve double resonance approaches which provide unique opportunities for isomer selective IR spectroscopy. This facet is among the advantages of gas-phase experiments, making it possible to follow certain properties, such as excited state dynamics, as a function of molecular structure. At the same time, the availability of gas-phase data provides opportunities to calibrate computational methods, force fields, and functionals.

2 Techniques

Gas-phase spectroscopy of neutral molecules, as opposed to ions, usually involves the use of supersonic molecular beams [1–4]. For smaller compounds this can be achieved by seeding in the inert drive gas. This limitation excludes the study of neutral nucleosides or larger compounds while even some of the bare nucleobases, such as guanine, cannot be sufficiently heated without thermal degradation. Some work with bases and base mimics has been done in seeded beams [5–10]. Larger compounds can now be vaporized successfully by pulsed laser desorption, followed by entrainment in a supersonic jet [11–14]. This experimental advance has opened up the field of study of nucleobases and nucleosides in isolation in the gas phase, especially by IR spectroscopy. The cooling in molecular beams makes this approach particularly attractive for spectroscopy. Although temperatures are not as low as in ion traps or helium droplets, molecular beams can achieve internal temperatures typically of the order of 10–20 K, which provides very useful optical resolution.

In a supersonic beam, typical densities are of the order of 10^{12} molecules/cm³. Therefore, at a typical absorption cross section of 10^{-18} cm², a 1-mm supersonic beam would absorb a fraction of 10^{-7} of incident photons. The low densities inherent in gas-phase experiments have led to the development and application of a number of suitable techniques in order to acquire infrared spectra.

2.1 *IR-UV Double Resonance*

Most of the work described in this chapter involves action spectroscopy in the form of IR-UV double resonance spectroscopy (DRS). In this approach, a secondary step reports on the absorption of the IR photon. A disadvantage is that the resulting spectrum is not a pure absorption spectrum but rather the composite result of two processes. An advantage can be that the secondary step can provide additional information. In the case of IR-UV double resonance, one combines direct IR absorption with either resonant two-photon ionization spectroscopy (R2PI) or laser induced fluorescence (LIF). A promising new variant is Ionization Loss Stimulated Raman spectroscopy [15]. The optical selection of the second step makes these techniques isomer-selective, which is their greatest strength. Comparison is sometimes possible with direct absorption techniques, although those generally lack isomer specificity, such as the following.

2.2 *Fourier Transform Microwave Spectroscopy*

In Fourier transform microwave spectroscopy, isomeric analysis is derived from rotational spectra; see [16]. Alonso and coworkers have combined this approach with laser desorption jet cooling for the study of tautomeric forms of nucleobases.

This technique identified tautomeric forms for all the canonical bases [17–20], as well as for several of their complexes with water [21], allowing comparisons with tautomer identifications from IR techniques.

2.3 Helium Droplets

In helium droplets, spectroscopy is usually performed in the infrared [22–25]. Resonant absorption by specific vibrational modes implies heating, resulting in helium atoms boiling off the droplets, recorded in a mass spectrometer or with a bolometer. The temperature in helium droplets is lower than in supersonic expansions and the cooling is so fast as essentially to freeze the starting population distribution. The starting temperatures need not be elevated much above room temperature because “pick-up” sources do not require very high gas densities.

2.4 Cavity Ringdown Spectroscopy and Multipass Absorption

Direct absorption probabilities can be enhanced by multipass arrangements and a particularly elegant and sensitive form of this principle is cavity ring down spectroscopy, where signal damping is recorded, rather than direct absorption. However, even at the largest ringdown times achievable with the highest quality mirrors, it is still difficult to measure IR absorption in a molecular beam. Saykally and co-workers obtained IR spectra of uracil and of nucleobase clusters with water by combining cavity ringdown and multipass spectroscopy with a slit nozzle, which produced an unusually wide molecular beam [26–28].

3 Monomers and Tautomeric Forms

The nucleobase monomers can adopt a variety of tautomeric forms and IR spectroscopy in the near IR is diagnostic for this property, especially with the NH and OH stretch frequencies as fingerprints of keto, imino, or enol forms.

3.1 Purines

For guanine, four species have been observed in R2PI spectra, labeled A–D, distinguished by UV–UV hole burning and characterized by IR–UV DRS

[29–35]. Figure 1e, g and h show experimental spectra from Nir et al., obtained by IR-UV DRS. Originally these tautomers were assigned as the four lowest energy forms, with A and D as enol forms and B and C as keto forms. The N7 vs N9 forms of each were subsequently distinguished by Mons et al. by selective methyl substitution [33]. However, the B, C assignment to the keto forms turned out to be incorrect. Surprisingly, these are imino forms, even though these tautomers are significantly higher in energy, and the three lowest energy tautomers are thus absent in the R2PI spectra, as described by Mons et al. and by Marian [36, 37]. This absence is explained by short, sub-picosecond, excited state lifetimes, to be discussed below, which render nanosecond timescales R2PI blind for these tautomers. The three “missing” tautomeric forms are shown in red in Fig. 1. Evidence that these tautomers are in fact present in the gas phase comes from two other

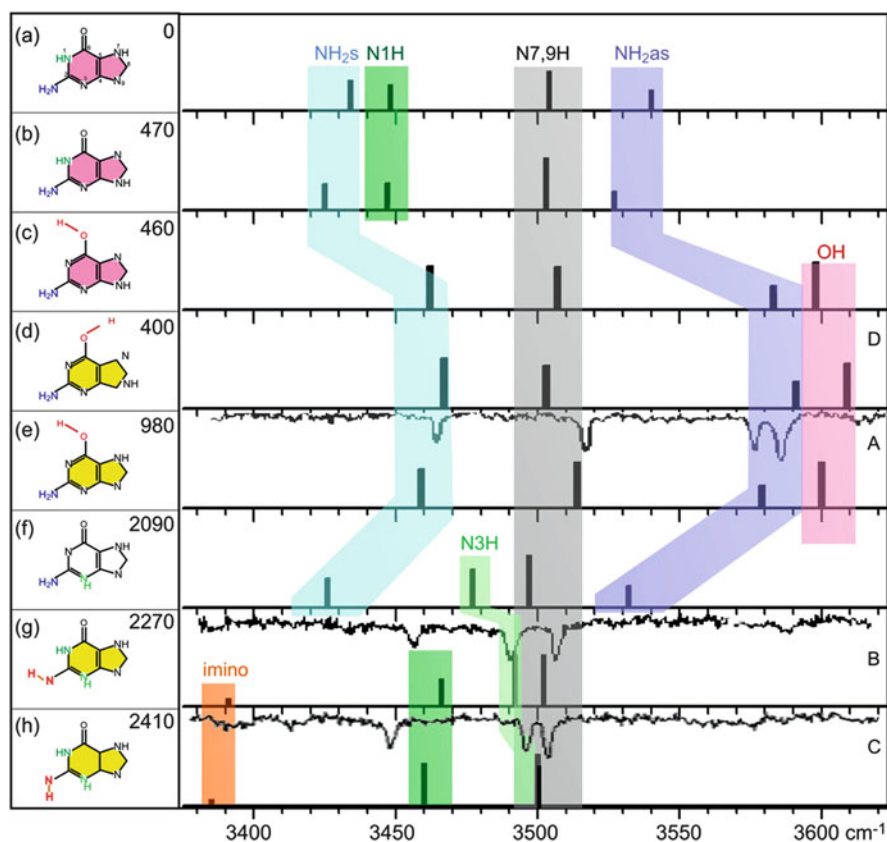


Fig. 1 a-h: IR frequencies for the eight lowest energy guanine tautomers, as calculated by Marian [36]. Modes are color-coded as shown in the structures on the left. Color coding of the structures is detailed in the text. Numbers are relative energies in cm^{-1} . e, g, and h show experimental IR-UV double resonance spectra from Nir et al. [29]. A–D refer to the four tautomers observed in R2PI spectroscopy

experiments which are direct absorption measurements, as opposed to action spectroscopy, and thus do not involve the excited state. One is FT microwave spectroscopy by Alonso et al., who observe the four lowest energy tautomeric forms (a)→(d) [19]. The second evidence comes from a helium droplet experiment by Choi and Miller who found the same four lowest energy tautomers [25]. These experiments are not isomer selective, so a large number of vibrational bands are observed in the infrared spectrum. The assignment was aided by aligning the molecules in an electric field and recording absorption as a function of the polarization angle of the light relative to the field. This elegant approach provides vibrational transition moment angles as additional data for comparison with *ab initio* theory.

Figure 1 shows IR frequencies for guanine as calculated by Marian [36]. The enol forms are characterized by the OH stretch at about $3,600\text{ cm}^{-1}$, marked in red, and a red shift of the symmetric and antisymmetric NH_2 stretches, marked in blue and purple, respectively. The imino forms are characterized by the imino NH stretch below $3,400\text{ cm}^{-1}$, marked in orange, which is, however, very low in intensity and therefore not diagnostic in most experimental spectra. The N1H and N3H stretches are marked in dark and light green, respectively. Pairs of tautomers which only differ in the N7H vs N9H forms, such as (a) vs (b) or (c) vs (e), have very similar IR signatures. The N7-H and N9-H frequencies are almost identical at about $3,500\text{ cm}^{-1}$, marked in gray. Sometimes tautomeric blocking by methyl substitution or deuteration can help resolve assignments [33, 34]. An analogous problem, which cannot be resolved by substitution, is the similarity in IR signature of conformational tautomers, such as (g) vs (h) or (c) vs (d). Because of this complication, assignments with complete confidence call for computational data at very high accuracy. This requirement is problematic, especially since currently available computations do not account for anharmonicity and thus employ scaling factors that are not rigorously defined.

Seefeld et al. confirmed the assignment of the B and C tautomers to the imino form by measuring the imino C=N stretch frequency at $\sim 1,700\text{ cm}^{-1}$ [38]. Figure 1 shows the resulting final assignments of the four long-lived tautomers A–D in yellow.

Nir et al. obtained IR-UV DRS spectra of a series of guanosines, some of which appear in Fig. 2 [29]. Figure 2a shows 9H enol guanine. The peak at $3,525\text{ cm}^{-1}$ marked in yellow corresponds to the N9H stretch and is absent in all the guanosine traces: 2',3'-deoxyguanosine (Fig. 2b), 3'-deoxyguanosine (Fig. 2c), 2'-deoxyguanosine (Fig. 2d), and guanosine (Fig. 2e). The blue and purple bands denote the symmetric and antisymmetric NH_2 stretch modes, while the red band denotes the OH stretch, showing that all these guanosines are in the enol form. As is the case with bare nucleobase, the keto form is not observed with nanosecond timescale R2PI. The red peaks correlate with the 2'-OH and the blue peaks correlate with the 3'-OH modes. The small red shift of the 3'-OH mode in Fig. 2e compared to Fig. 2d indicates a small amount of hydrogen bonding, consistent with a “windshield wiper” orientation with the 3'-OH pointing towards the 2'O. The 5'-OH frequency is absent in this frequency range, presumably because of strong red shifting, suggesting a strong

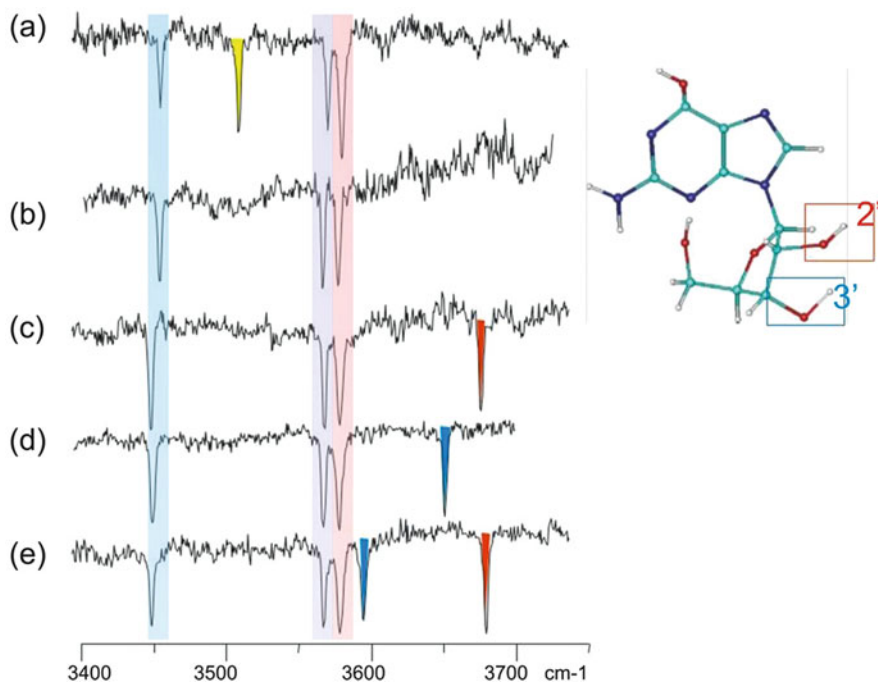


Fig. 2 IR-UV DRS spectra of (a) guanine, (b) 2',3'-deoxyguanosine, (c) 3'-deoxyguanosine, (d) 2'-deoxyguanosine, and (e) guanosine

internal hydrogen bond consistent with a *cis* orientation of the sugar. In the biological context this hydrogen bond is absent. Asami et al. have shown that, while indeed the *cis* form is most stable, by contrast, in the case of 5'-*O*-ethylguanosine, the anti conformer is stabilized by the formation of hydrogen bonding involving the 2'-OH group [39, 40].

The near IR range between 3,000 and 4,000 cm^{-1} is very diagnostic for structure since it contains the N-H and O-H stretches. Inclusion of the C=O stretch frequency around 1,800 cm^{-1} , which now becomes possible with table-top laser systems, extends the useful range further. The mid-IR range, typically 500–2,000 cm^{-1} , attainable with a free electron laser, usually does not add much extra structural information. Those lower frequency modes can add further detail, however, especially for the sugar in nucleosides. Figure 3 shows IR-UV DRS spectra obtained at the FELIX free electron laser facility of guanosine (Fig. 3a) and 2'-deoxyguanosine (Fig. 3b) [41]. The red peaks correspond to modes in the guanine, while blue colored peaks denote modes of the sugar moiety. Figure 3c shows the spectrum of 9-ethyl-guanine for comparison, with the main ethyl modes marked in yellow.

The tautomeric landscape of adenine is somewhat less varied than in the case of guanine because of the absence of the oxygen. Plützer and Kleinermanns reported IR-UV double resonance and observed two tautomers, for which Fig. 4 shows the

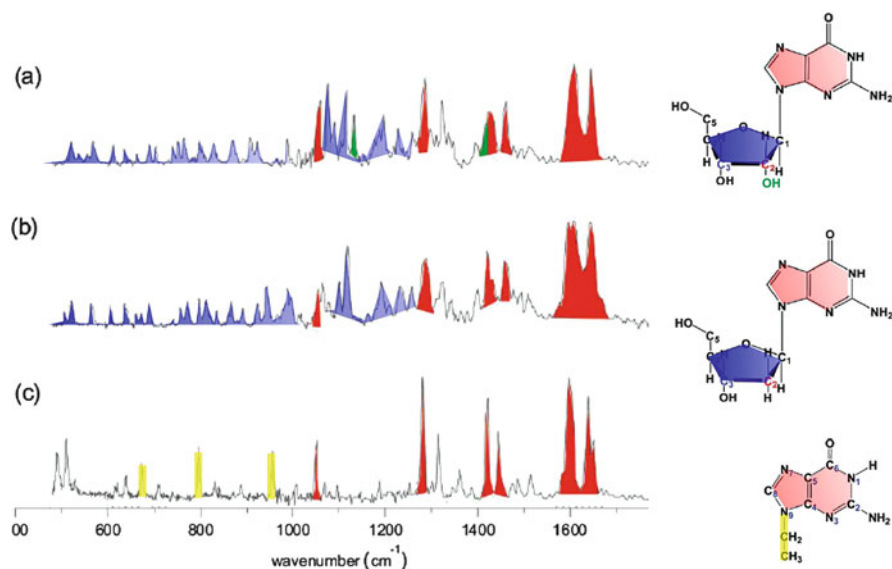


Fig. 3 IR-UV DRS spectra of (a) guanosine, (b) 2'-deoxyguanosine, and (c) 9-ethyl-guanine

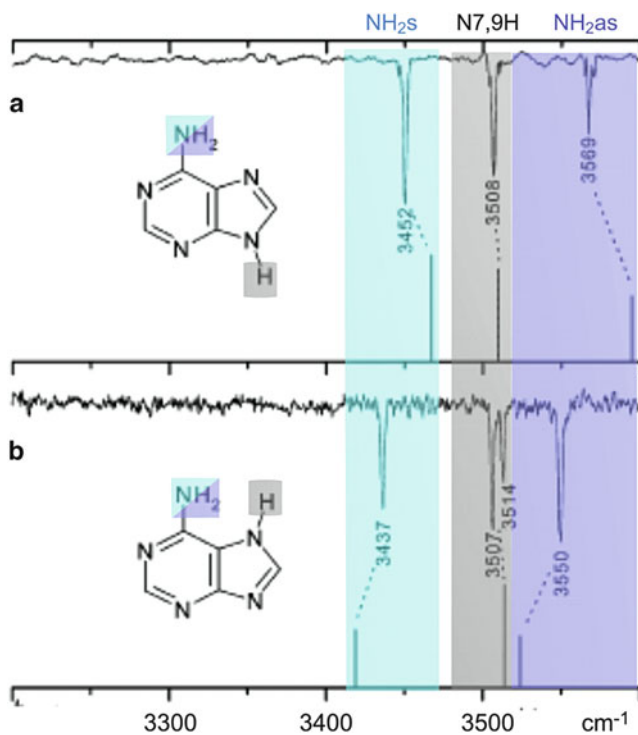


Fig. 4 IR-UV double resonance spectrum of adenine with the R2PI laser tuned to (a) $36,105 \text{ cm}^{-1}$ and (b) $35,824 \text{ cm}^{-1}$. The *stick spectrum* shows the vibrational frequencies calculated at the B3LYP/6-311G(d,p) level. Data from Plützer and Kleinermanns (reprinted with permission, color coding added) [42]. Stick spectra were computed at the B3LYP/6-31G(d) level with a scaling factor of 0.9613

IR spectra [5, 42]. Both tautomers are of the amino form, with the *9H* form by far the most abundant relative to the *7H* form. This finding is consistent with the microwave measurements by Brown et al. [43]. At the conditions of jet cooling, the imino form appears to be absent, although in the gas phase at elevated temperature the IR spectra seem to comprise multiple tautomers, including imino. The analysis is somewhat complicated by the fact that the UV spectra contain contributions to two excited states, of $\pi\pi^*$ and $n\pi^*$ character, respectively [44, 45].

3.2 Pyrimidines

Figure 5 displays the main tautomers observed for the pyrimidine bases. Cytosine appears in both the keto and enol form, while uracil and thymine each appear almost exclusively in the diketo form. The IR-UV DRS spectrum of keto-cytosine appears in Fig. 6a, with 1-methyl and 5-methyl derivatives for comparison in Fig. 6b, c, respectively. The two enol forms for cytosine cannot be distinguished realistically by available IR spectra. The enol tautomer is slightly more stable than the keto form by about 0.03 eV [46–48]. The keto form is the biologically important one, with Watson–Crick base pairing in DNA, and predominant in solution. The keto-imino form in cytosine is much higher in energy. In matrix isolation, Szczesniak et al. observed both keto and enol forms with higher abundances for the latter and small contributions from the imino form [49]. Brown et al. have obtained rotational constants for all three tautomeric forms by microwave spectroscopy [50].

While the energy difference between the enol and keto forms is very small, some of their other properties, such as their vertical excitation energies, are very different [51]. Nir et al. reported R2PI and hole burning spectra and concluded that the keto and enol tautomers have band origins which differ by a remarkable half an electron volt at 314 and 278 nm, respectively [52, 53]. The R2PI spectra of U and T exhibit a very broad structure with an onset in the frequency range of the origin of the enol cytosine first reported by Brady et al. [4]. No spectroscopic detail could be extracted

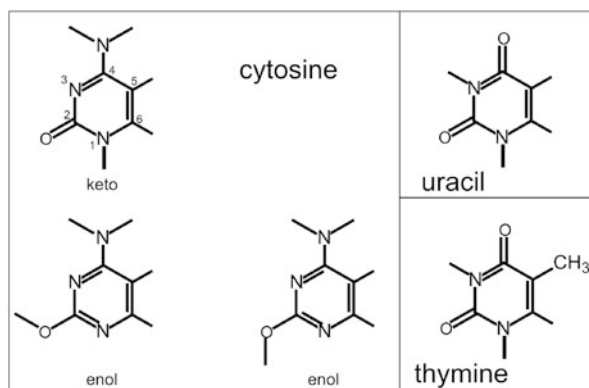


Fig. 5 Structures of lowest energy tautomers of the canonical pyrimidine bases

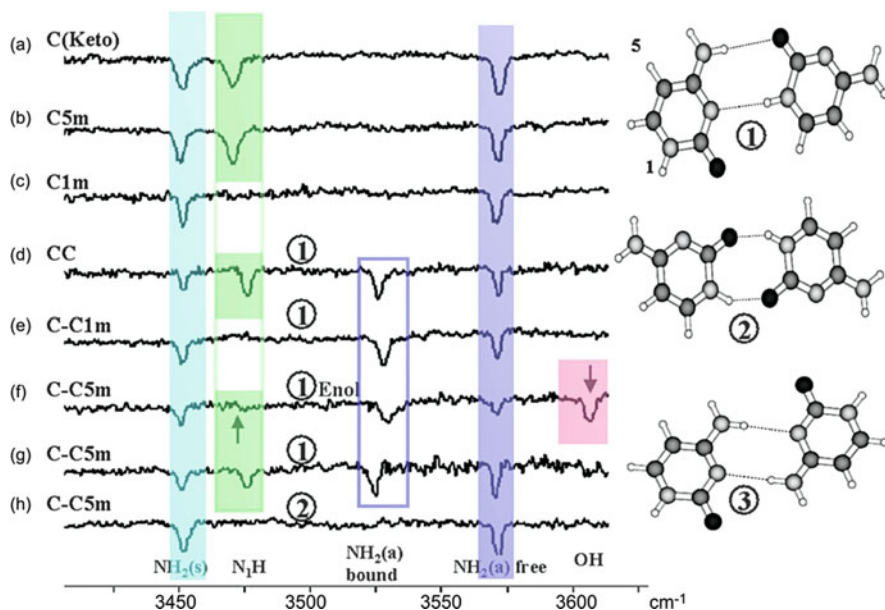


Fig. 6 IR-UV DRS spectra of cytosine monomers (a–c) and dimers (d–h). C1m and C5m denote 1-methylcytosine and 5-methylcytosine, respectively. *Circled numbers* on the dimer traces refer to the cluster structures shown on the right. (f–h) were recorded at three different UV wavelengths, corresponding to three different structures of the C-C5m cluster

from these broad spectra and tautomeric information was limited for a long time to bulk measurements.

Microwave measurements of uracil in a heated cell suggested the diketo form as the most abundant [54]. Brown et al. reported the first microwave measurements in a seeded molecular beam and also concluded that the diketo form was predominant [55]. Viant et al. reported the first rotationally resolved gas phase IR spectra of uracil [28]. This work employed a slit nozzle, an IR diode laser, and a multipass arrangement to obtain high resolution IR absorption spectra of the out-of-phase $\nu_6(\text{C}_2=\text{O}, \text{C}_4=\text{O})$ stretching vibration. The rotational analysis unambiguously assigned the species to the diketo tautomer. Brown et al. also observed the diketo form of thymine in a seeded molecular beam, based on the hyperfine structure in the $14_{4,10}-13_{3,11}$ transition [56].

Recently, Ligare et al. confirmed the diketo character of the broad absorption of both U and T by IR-UV DRS. Their spectra showed ion gain rather than dips upon IR excitation. Double resonant spectroscopy relies on the fact that the burn laser changes the ground state vibrational distribution and thus the overall Franck–Condon (FC) factors. When the probe laser is tuned to a strong resonance, this invariably leads to ion dip. However, in the case of a broad absorption, the consequences of modified FC factors are not always predictable and an ion dip may not necessarily occur. In the case of U and T, it is probable that there is a large

geometry change between the ground state and the excited electronic state, which leads to more favorable FC factors and thus ion gain. Such a scenario would also help explain the gradual onset of the R2PI spectrum and the absence of a strong 0–0 transition.

3.3 Excited State IR

An additional reason for excited state broadening may be lifetime broadening. As discussed below, most of the $\pi\pi^*$ excited state returns to the ground state on a picosecond timescale by internal conversion. However, there is a small quantum yield for a process leading to a “dark” excited state of $n\pi^*$ character or a triplet state ($^3\pi\pi^*$ or $^3n\pi^*$). Kunitski et al. have characterized this dark state for 1-methylthymine by performing IR-UV DRS on the excited state, rather than the ground state [57]. Figure 7 shows the spectra obtained for the NH stretch. The bottom trace is the usual ground state IR-UV DRS spectrum. The top trace results from a different pulse sequence in which the molecule is first excited by the pump laser and partly relaxes into the dark state, which is subsequently subjected to be IR burn pulse and ionized by the probe pulse. The result is a small red shift, interpreted as characteristic for a triplet state, whereas an $n\pi^*$ state would have produced a blue shift. Ligare et al. have recently obtained similar results for thymine itself.

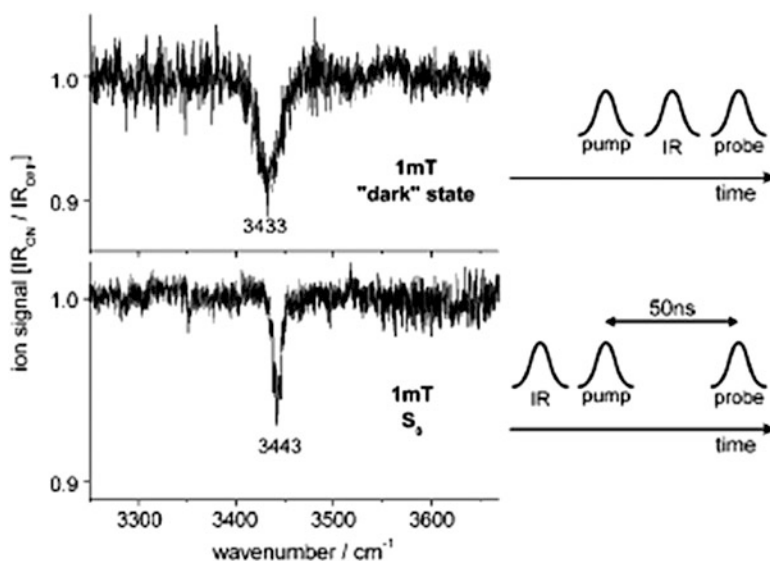


Fig. 7 Ionization-detected IR spectra of 1-methylthymine in the ground state (*bottom*) and long lived transient excited state (*top*) in the NH/OH stretch region. The corresponding laser pulse sequences are shown on the *right* [57]

3.4 Ionic Nucleobases and Nucleotides

For nucleotides, the charge on the phosphate group generally precludes the use of the IR-R2PI hole burning technique. Instead, it is possible to study ions in a trap by IR multiphoton dissociation (IRMPD). The characteristics of a free electron laser, such as FELIX, with its macro and micro pulses, are very suitable for this type of multiphoton IR spectroscopy [58]. Since there is no isomer selection in this case, the interplay with theory is especially important and the occurrence of multiple structural forms could complicate interpretation. van Zundert et al. compared results for neutral (by DRS) and protonated (by IRMPD) adenine and 9-methyladenine in the same mid-IR frequency range of 525–1,750 cm^{-1} [59]. They found the 9H tautomer to be dominant for both neutrals and ions. Salpin et al. studied protonated uracil, thymine, and cytosine by IRMPD spectroscopy [60]. Calculated infrared frequencies of the different low-lying isomers (computed at the B3LYP/6-31++G4CHTUNG TRENUNG(d,p) level) predict the global energy minimum for an enolic tautomer in each case, whose infrared absorption spectra matched very well with the experimental IRMPD spectra. An additional very weak IRMPD signal observed at about 1,800 cm^{-1} suggests the presence of the second lowest energy oxo tautomer. Oomens et al. studied protonated cytosine dimers, concluding that the proton moves from one basic atom to another when the dimer ion dissociates [61]. Yang et al. studied the effect of C5 substituents on the cytosine base pairing motifs and concluded that the substitution does not alter the lowest energy base pairing structures [62, 63]. Yang et al. found a single tautomer for alkali metal cation cytosine complexes [64], as did Nei et al. for sodiated uracil and thiouracil complexes [65, 66]. On the other hand, Crampton et al. found that protonation preferentially stabilizes minor tautomers of halouracils [67].

Nei et al. have reported the IR spectra of all deprotonated canonical nucleotides, trapped in an FTICR instrument and subjected to IRMPD in the mid-IR [68, 69]. The measured IRMPD action spectra were compared to the linear IR spectra calculated at the B3LYP/6-311+G(d,p) level of theory and the most stable conformations of the deprotonated forms of dA5'p, dC5'p, and T5'p were found to be conformers where the ribose moiety adopts a C3' *endo* conformation and the nucleobase is in an *anti* conformation. By contrast, the most stable conformations of the deprotonated form of dG5'p are conformers where the ribose adopts a C3' *endo* conformation and the nucleobase is in a *syn* conformation. In addition to the ground-state conformers, several stable low-energy excited conformers that differ slightly in the orientation of the phosphate ester moiety were also accessed in the experiments. Comparison of the conformations found by these authors for DNA nucleotides vs RNA nucleotides would suggest that the intrinsic difference between the DNA and RNA mononucleotides is probably not caused by their relative conformations but by the change in their chemical properties induced by the different substituents at the C2' position [68]. By the same technique, Ligare et al. studied deprotonated clusters of nucleotides and found that, unlike in multimer double stranded DNA structures, the hydrogen bonds in these isolated

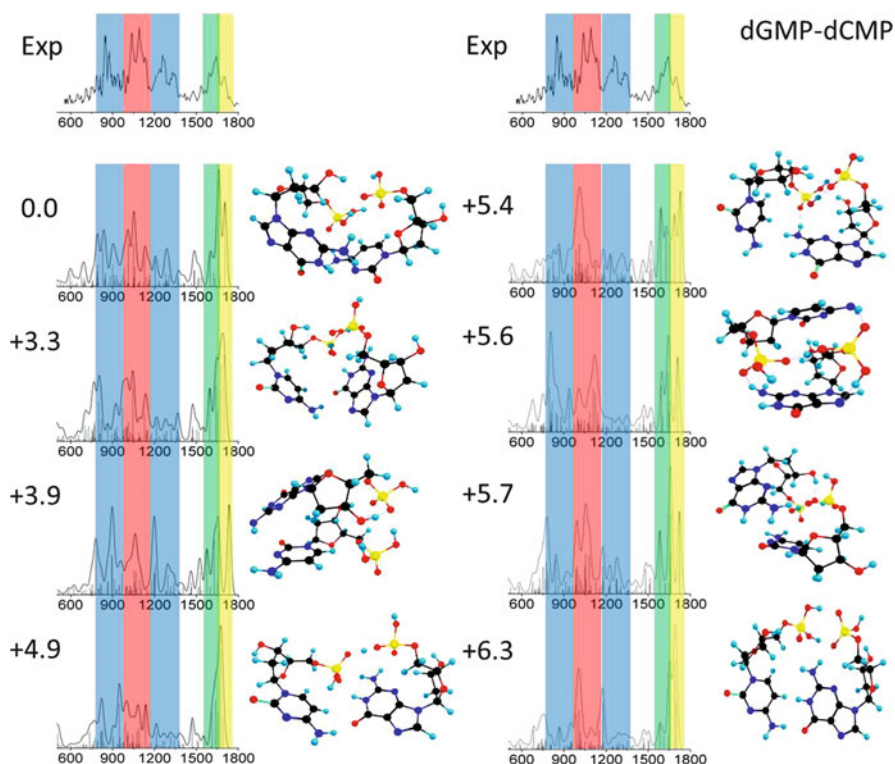


Fig. 8 The six lowest calculated energy spectra for deprotonated [dGMP-dCMP]- compared with IRMPD experiment. The energies listed are Gibbs free energies in kcal/mol relative to the ground state structure [70]

nucleotide pairs are predominantly formed between the phosphate groups, as shown in Fig. 8.

4 Cluster Structures

IR spectroscopy is also very diagnostic for the structure of hydrogen bonded clusters. Upon hydrogen bonding, NH and OH stretch frequencies in the near IR generally shift to the red, often by hundreds of wavenumbers, while also broadening. The extent of the red shift is correlated with the strength of the hydrogen bond. The red shift and broadening cannot be computationally predicted with much accuracy, although they are very clear indicators, showing which hydrogen bonding sites are implicated in bonds, while frequencies that do not shift mark the free sites. Therefore near IR spectra can provide insight into the cluster structure, often to the point of complete structural assignment.

4.1 Base Pairs

Figure 6 demonstrates this principle for cytosine dimers. Figure 6c–g, with both a free and a bound (shifted) NH_2 vibration clearly point to structure 1. Figure 6h with only free NH_2 is consistent with structure 2, while structure 3 can be excluded for all of these spectra, since it would contain no free NH_2 modes. Furthermore, the $3,600\text{ cm}^{-1}$ OH frequency, characteristic for the enol form, appears only in Fig. 6f.

Figure 12 shows IR-UV spectra for three structural isomers of GC base pairs [72]. The stick spectra are DFT calculated vibrational frequencies for the structures shown in the insets. Structure A is the Watson–Crick structure, while structure C is almost the same structure, although the cytosine is in the enol form instead of in the keto form. This subtle tautomeric difference has a dramatic effect on the photophysical properties as discussed below. The IR-UV spectrum in F correlates with a broad, structureless UV spectrum. The fact that broad UV absorption yields a sharp IR-UV hole burning spectrum is somewhat fortuitous. The IR burn pulse excites a specific vibrational mode around $3,000\text{ cm}^{-1}$, followed by internal vibrational redistribution (IVR) on the picosecond timescale. The resulting vibrational state populations produce a different Franck–Condon landscape, which for a broad absorption may or may not lead to depletion of the UV probe signal. In fact, it is possible that the new FC landscape leads to a gain in ionization signal, as observed for uracil and thymine. Mayorkas et al. also observed gain signals in ionization loss stimulated Raman spectroscopy of tryptamine conformers [73]. Similarly, gain signals are possible following excitation in the mid-IR, which imparts a small amount of energy and thus provide less opportunity of vibrational redistribution.

A particular computational challenge is the incorporation of anharmonicity of the potentials. A common fix is the application of scaling factors but this approach, while useful, is clearly fraught with uncertainty. While it is good practice always to use the same empirical factor for consistency, it is also reasonable to assume that different modes could require different factors, leaving one with a somewhat uncomfortable number of empirically adjustable parameters. In the quest to develop more comprehensive computational strategies, it is useful to be able to compare with both near- and mid-IR data as sensitive tests. Figure 9 shows such a comparison for the GC base pair with the cytosine in the enol form, as depicted in Fig. 12c [74]. The mid-IR part of this spectrum (left panel) was obtained at FELIX and the lower frequencies provide an especially sensitive test for theory. Comparison of the theoretical frequencies with the experimental results indicates that the average absolute percentage deviation for the methods is 2.6% for harmonic RI-MP2/cc-pVDZ (3.0% with the inclusion of a 0.956 scaling factor which compensates for anharmonicity), 2.5% for harmonic RI-MP2/TZVPP (2.9% with a 0.956 anharmonicity factor included), and 2.3% for adapted PM3 CC-VSCF; the empirical scaling factor for the ab initio harmonic calculations improves the stretching frequencies but decreases the accuracy of the other mode frequencies.

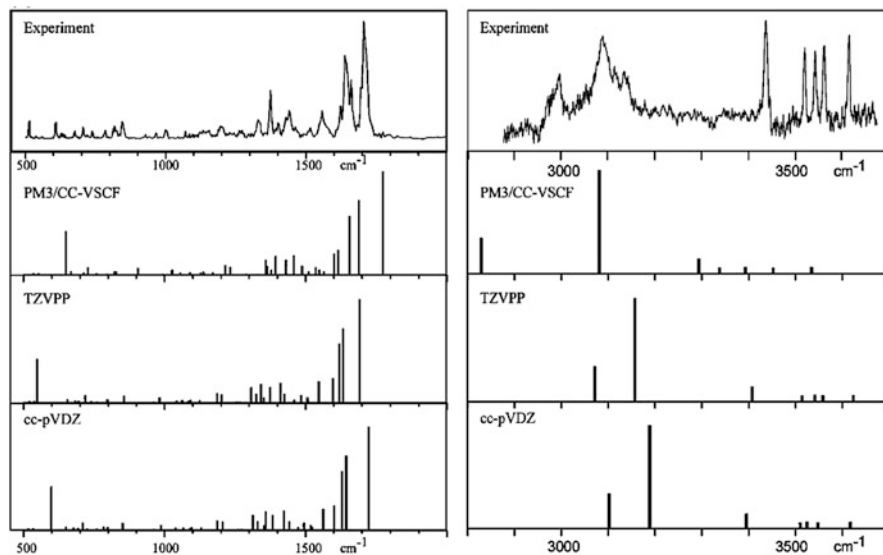


Fig. 9 Comparison of experimental data with calculations according to different models aimed at correcting for anharmonicity [74]

This work is an example of the ongoing cross fertilization of theory and experiment, in which gas-phase data serve as benchmarks for computational method development, while the computations provide the analysis of the experimental results.

For AT base pairs, Plützer et al. reported the IR-UV spectrum, which they assigned to cluster structures with $(\text{HNHO})\text{-O}\cdots=\text{C}(\text{NHN})\text{-H}\cdots$ hydrogen bonding by comparison with ab initio calculated vibrational spectra of the most stable A–T isomers [75]. The Watson–Crick A–T base pair is not the most stable base-pair structure at different levels of ab initio theory, and its vibrational spectrum is not in agreement with the observed experimental spectrum. This is directly shown by the free N3H vibration in the IR spectrum of AT. This group is involved in hydrogen bonding in the Watson–Crick pair. Experiments with methylated A and T further support the structure assignment.

4.2 Clusters with Water

IR-UV DRS also lends itself to analysis of clusters with water in order to study the details of hydration, one water molecule at a time. Figure 10 shows IR-UV spectra of guanine water clusters as an example [76]. Figure 10a–c shows spectra from three observed structures while Fig. 10d–f show spectra from corresponding non-hydrated structures for comparison. The hydrated spectra contain broad, red-shifted peaks caused by hydrogen bonded modes, but the free modes suffice

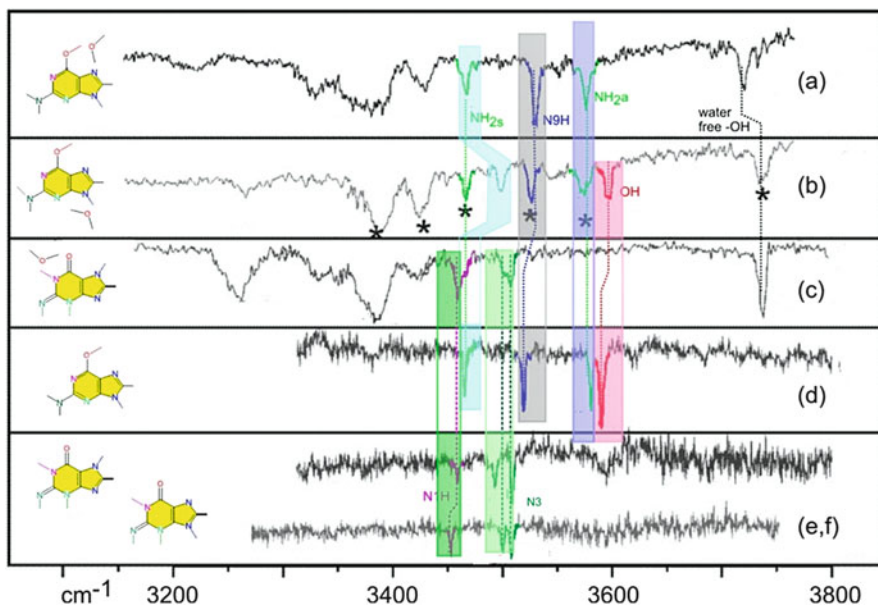


Fig. 10 IR-UV hole burning spectra of guanine with (a–c) and without (d–f) water. Corresponding modes for corresponding structures with and without water are indicated by *dotted lines* and color coding. Structures are schematic only. *Asterisks* denote peaks in **b** which also show up in **a**, probably caused by overlap in the probe spectra. Adapted from [76]

for analysis. They each contain a free water OH stretch, excluding bridged structures. Figure 10a, b parallel Fig. 10d. Figure 10b contains the free enol OH mode. Figure 10a is almost identical but without the enol OH mode indicating an enol with the water bound to the OH. Figure 10c parallels Fig. 10e, f, missing both NH_2 modes as well as the enol mode, but showing the N3H and N1H mode characteristic for the imino form. Once again, the keto form is not observed in these experiments. Chin et al. also reach that conclusion in their detailed study of rotamers of 9-methylguanine with water [32, 35].

Saigusa et al. reported IR-UV DRS spectra of hydrated clusters of nucleosides [77, 78] and of GG and GC base pairs [79]. For the monohydrated cluster of Gs they found multiple structural isomers. For one of the monohydrates they assigned a hydration structure involving the 5'-OH group of the sugar and the amino group of the guanine moiety. From the IR spectrum of the dehydrated clusters they inferred that the 2'-OH group is significantly influenced by the addition of the second water, which suggests the possibility of specific dihydrate structures for Gs. Their results also suggest that the amino-keto forms of Gs and 9MG, which are missing in the R2PI spectrum, can be observed upon hydration.

4.3 Stacking vs H-Bonding Structures

Two structural motifs dominate in DNA: π -stacking provides most of the structural stability of the helix while hydrogen bonding provides most of the recognition properties. For pairs of single bases H-bonding is the exclusive motif in the gas phase, while stacking dominates in solution. Water molecules stabilize the stacked structure both by competing with hydrogen bonding sites on the bases and by stabilizing the structure by forming bridges. Hobza and coworkers have calculated how many water molecules are needed to lead to preferential stacking and concluded that, depending on the base pair, this number can range from two to five [80, 81]. Clusters of that size have not yet been characterized in the gas phase, so this transition has not yet been experimentally verified. Another way to encourage stacking is blocking hydrogen bonding sites by methylation and several examples have been reported.

Callahan et al. have used xanthine and its methylated derivatives as models for studying the two motifs [82, 83]. For the 7-methylxanthine dimer, they observed hydrogen bonding on the N3H position, suggesting three possible combinations, one that is reverse Watson–Crick type and two that are reverse Hoogsteen type. For the 3–7-dimethylxanthine dimer, they observed a stacked structure, as determined by the free N1H stretch frequency. For trimethylxanthine dimers they inferred a stacked structure as well.

Plützer et al. reported a stacked structure for 9-methyladenine-adenine (9 mA-A) clusters based on one free NH_2 group and one weakly interacting NH_2 and N9H group in the IR-UV spectrum [84]. They found no evidence of stacking for A-A, 7 mA-A, or 9 mA-9 mA clusters. The latter shows only broad vibronic structure and is probably symmetrically hydrogen bound via the NH_2 groups. Interestingly, the symmetrically bound A-A cluster structure was not observed, although it is predicted to be the lowest in energy. Smith et al. studied adenine and microhydrated $A_m(\text{H}_2\text{O})_n$ clusters by femtosecond pump–probe mass and photoelectron spectroscopy [85]. For the predominantly hydrogen-bonded adenine dimer, excited state relaxation is dominated by monomer-like processes. However, when the adenine dimer is clustered with several water molecules, they observed a nanosecond lifetime ascribed to excimer states in π -stacked clusters.

Asami et al. reported IR-UV DRS spectra for base pairs of adenine nucleosides, adenosine (Ado) and *N*6,*N*6-dimethyladenosine (DMAdo) [77]. They found that the dimer possesses a stacked structure, stabilized by the formation of a hydrogen-bonding network involving the two sugar groups. The occurrence of the frequency shift and broadening is explained satisfactorily based on the anharmonic coupling of the OH stretching modes with specific bending modes and low-frequency modes of base and sugar moieties. By contrast, Saigusa et al. performed experiments with GG and GC pairs with methyl substitutions in the sugar position, which for GC forces the Watson–Crick structure. The IR markers for this structure remained essentially unchanged upon hydration, suggesting no significant structural change nor stabilization of π stacking [79].

5 Excited State Dynamics

With the ability to perform isomer-selective IR spectroscopy has come the opportunity to study effects of subtle structural variations. One of the remarkable outcomes is that certain low energy isomers have not been observed in IR-UV DRS. Notable examples are the keto tautomer of guanine and the Watson–Crick structure of the GC base pair. Similarly, the lowest energy symmetrically hydrogen bonded structures of homodimers, such as GG and AA, are missing in these IR-UV measurements. Intriguingly, these “missing” isomers tend to be the biologically most relevant forms. Inevitably, double resonant spectroscopy involves a form of action spectroscopy, usually two-photon ionization and sometimes laser induced fluorescence. Both techniques detect the excited state. In a number of cases, where direct absorption measurements are available, the “missing” isomers are in fact observed, implying that they do exist in the gas phase. A prime example is the keto tautomer of guanine, which is identified both in microwave spectroscopy in a molecular beam [19] and in helium droplets [25].

The failure to observe certain isomers can be attributed to short-lived electronically excited states. An excited-state lifetime of the order of picoseconds or less is in fact four or more orders of magnitude shorter than the typical laser pulses of several nanoseconds, routinely used for two-photon ionization. This fact renders this form of action spectroscopy blind for the species with the shortest excited state lifetimes. A picture is now emerging in which the electronic excited state can undergo rapid internal conversion to the ground state. The key is the occurrence of conical intersections (CIs) which connect the excited state potential energy surface, reached by photon absorption, to the ground state potential energy surface. The dramatic lifetime differences between isomers and derivatives of nucleobases appear to be caused by variations in the excited state potential surfaces which restrict or slow access to these conical intersections [86]. As illustrated schematically in Fig. 11, conical intersections are the crossings of multidimensional potential surfaces. Therefore, these features can only occur in regions of the potential energy landscape which represent a deformation of the molecular frame from the ground state equilibrium geometry. For example, Fig. 11 shows the geometry at the conical intersection for the keto tautomer of guanine, calculated by Marian [36]. The CI involves strong out-of-plane bending of the C2 coordinates and different tautomeric arrangements lead to different potential surfaces along those coordinates. As a result, other tautomers do not lead to the same trajectories on the excited state potential surface and only the keto form exhibits the barrierless pathway through the CI, producing its sub-picosecond internal conversion. This mechanism also explains the strong dependence of excited state lifetimes on derivative structure [87–89]. When a subpicosecond internal conversion pathway is available (indicated schematically in red in Fig. 11), it can compete favorably with other processes, such as fluorescence (green) or other photochemical processes (orange).

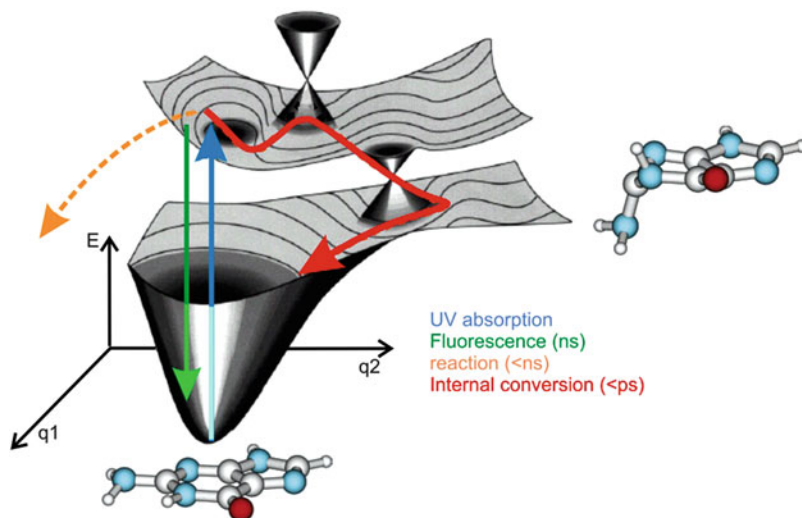


Fig. 11 Schematic potential energy diagram as a function of two generic internuclear coordinates, q_1 and q_2 , showing the concept of conical intersections connecting different electronic states. *Insets* show the geometry of guanine at the ground state equilibrium and at the conical intersection between the $\pi\pi^*$ and the SO state, as calculated by Marian [36]

In the case of the pyrimidine bases, the major coordinates forming the CI are torsion and stretching of the C5=C6 bond. For 4-aminopyrimidine, surface hopping calculations identified two conical intersections [5, 42, 45, 90–101]: deformation at the C2 position leads to deactivation of the excited state with a lifetime, τ^* , of 1 ps and deformation at the C5=C6 bond with a τ^* of 400 fs. Immobilizing the latter with a 5-membered ring forms adenine with a conical intersection produced by the C2 deformation, τ^* , of 1 ps and dynamics similar to that in guanine. C2 substitution changes the potential energy landscape along this coordinate, such that adenine's isomer 2-aminopurine has a nanosecond excited state lifetime and strongly fluoresces. Similarly, for the pyrimidine bases the oxygen substitution at the C2 position eliminates the CI associated with the C2 puckering but leaves the CI associated with the C5=C6 coordinates available for internal conversion. C5 substituents in pyrimidines further alter excited state lifetimes over a range of picoseconds to nanoseconds by modification of the topography of the potential energy surfaces around C5=C6 torsion and stretching coordinates [89, 102, 103]. Interestingly, the same coordinates are found to play a role in thymine photo-dimerization in DNA [104].

We can now rationalize why, for GC clusters, the one structure that is prevalent in DNA, the Watson–Crick structure, has not yet been observed by two-photon ionization with nanosecond laser pulses. In the work of Nir et al. only a substituted version (9-ethyl-G-1-methyl-C) was reported (Fig. 12a), and its corresponding two-photon UV spectrum was very broad [72, 105]. Presumably, the Watson–Crick structure has a sub-picosecond excited state lifetime, while other structural

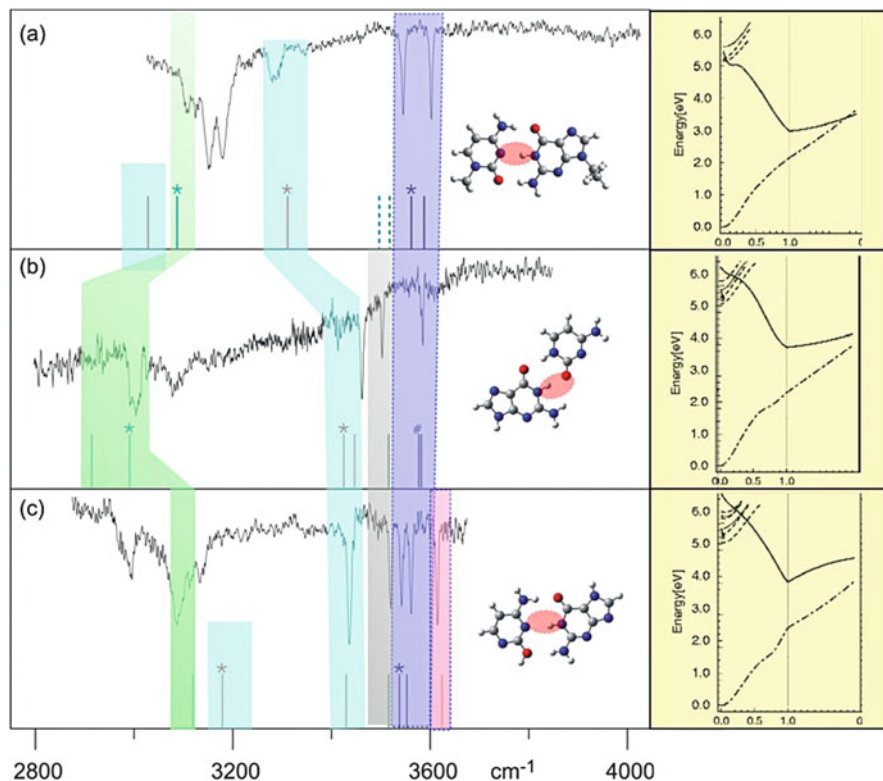


Fig. 12 Left column shows three structures observed for isolated GC base pairs, as identified by IR-UV spectroscopy. Stick spectra are DFT calculated vibrational frequencies. Structure A is the Watson–Crick structure. Right column shows calculated potential curves [71]. A charge transfer state (CT in red) connects the S1 (green) and S0 state (blue) by two conical intersections in (a) but not in (b) and (c). The reaction coordinate is middle hydrogen motion, N1-H, indicated with a red ellipse in the structures. Color coding of the modes is the same as in Fig. 1

arrangements of the same base pair have sharp spectra, consistent with much longer excited state lifetimes [106]. To explain the effect, the right column of Fig. 12 shows calculated potential curves from Sobolewski and Domcke [71]. The reaction coordinate is hydrogen motion, N1-H, indicated with a red circle in the structures. A charge transfer state connects the S1 and S0 states by two conical intersections in A but not in B and C. The difference in tautomeric form between the A and the C case induces a subtle change in the excited state potential energy landscape. The charge transfer state is just slightly higher in energy relative to S0 and S1, creating a barrier for reaching the first conical intersection. Thus a small change in potential energies upon tautomerization results in a difference of orders of magnitude in excited state lifetime.

It has been argued that a short excited state lifetime, by virtue of rapid internal conversion, is nature’s strategy to protect the building blocks of life against UV

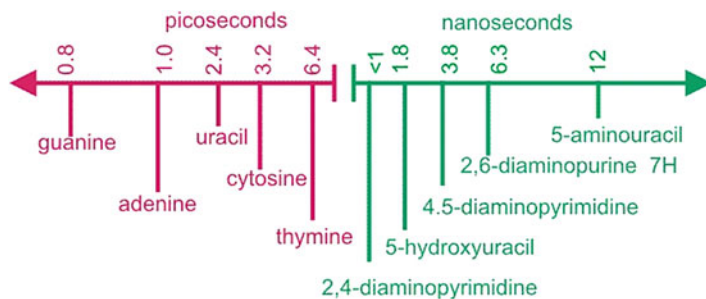


Fig. 13 Representative excited state lifetimes in the gas phase

induced damage which would otherwise result from slower photochemical processes. Figure 13 shows excited state lifetimes for the canonical bases in comparison with those for several of their derivatives. It appears that sub-picosecond lifetimes are a fairly unique property of the canonical bases and, as outlined above, this property is even specific to tautomers and base pair structures encountered in DNA. This would, however, not be a strategy that could have been adopted by biological evolution. For evolution to proceed, the replication machinery has to be in place first. Therefore, any photochemical properties the bases have, must have originated from prebiotic times. Assuming that a primordial soup would have contained many possible variations of the heterocyclic compounds, it is conceivable that the building blocks of life underwent photochemical selection on an early Earth. If so, these properties would be relics from chemistry that took place some four billion years ago.

In this context, it needs to be remembered that gas-phase spectroscopy constitutes a reductionist approach to the study of basic chemistry. Extrapolation to bulk conditions requires consideration of hydrogen bonding and stacking interactions. These interactions modify the photochemistry. For example, π stacking can lead to exciplex formation, which opens up additional deexcitation channels [107].

6 Summary and Outlook

The prime objective of gas-phase studies is the investigation of intrinsic properties in *isolated* molecules. For a long time this approach has been limited to small molecules. The application to larger molecules is made possible by simultaneous progress in both experimental and computational technique. Laser desorption has made it possible to vaporize low vapor pressure neutral compounds intact and progress in computing power and theoretical treatments have made larger systems amenable to high level computation. The resulting interplay between theory and experiment has been a powerful driver of this field of study. Theory has been instrumental in analyzing and guiding experiments, while at the same time

gas-phase data are valuable for calibrating computational strategies. IR frequencies are among the best experimental data, available for this purpose. IR-UV DRS has emerged as a particularly fruitful meeting ground between theory and experiment, given its isomer selectivity. At this point, even very high level computations still lack precision, particularly in predicting hydrogen bond shifts and accounting for anharmonicity, so progress on this front may still be expected. It is still unclear what the molecular size limit is for this approach. The extrapolation from isolated molecules to bulk is probably aided by studies of clusters. In addition to base pair clusters, work on several small clusters with water has been reported, but data on larger clusters, at least approaching a first solvation shell, are still desirable.

A major use of IR data is structure determination, which for nucleobases includes tautomeric forms and cluster structures to model base pair interactions and microhydration. This capability also makes it possible to follow other properties as a function of structure. For the nucleobases, it turns out that self-protection against UV photodamage by internal conversion depends dramatically on molecular structure. Comparison with solution experiments probably further elucidates these findings and stimulates further research.

Acknowledgement This material is based upon work supported by the National Science Foundation under CHE-1301305 and by NASA under Grant No. NNX12AG77G.

References

1. Kim SK, Lee W, Herschbach DH (1996) Cluster beam chemistry: hydration of nucleic acid bases; ionization potentials of hydrated adenine and thymine. *J Phys Chem* 100:7933–7937
2. Anderson JB, Fenn JB (1965) Velocity distributions in molecular beams from nozzle sources. *Phys Fluids* 8:780
3. Levy DH (1980) Laser spectroscopy of cold gas-phase molecules. *Annu Rev Phys Chem* 31:197–225
4. Brady BB, Peteanu LA, Levy DH (1988) The electronic spectra of the pyrimidine bases uracil and thymine in a supersonic molecular beam. *Chem Phys Lett* 147:538–543
5. Plützer C, Nir E, de Vries MS, Kleinermanns K (2001) IR-UV double-resonance spectroscopy of the nucleobase adenine. *PCCP* 3:5466–5469
6. Muller A, Talbot F, Leutwyler S (2000) Intermolecular vibrations of jet-cooled (2-pyridone)/sub 2/: a model for the uracil dimer. *J Chem Phys* 112:3717–3725
7. Muller A, Talbot F, Leutwyler S (2001) Intermolecular vibrations of the jet-cooled 2-pyridone center dot 2-hydroxypyridine mixed dimer, a model for tautomeric nucleic acid base pairs. *J Chem Phys* 115:5192–5202
8. Muller A, Talbot F, Leutwyler S (2002) Hydrogen bond vibrations of 2-aminopyridine center dot 2-pyridone, a Watson–Crick analogue of adenine center dot uracil. *J Am Chem Soc* 124:14486–14494
9. Frey JA, Muller A, Frey HM, Leutwyler S (2004) Infrared depletion spectra of 2-aminopyridine center dot 2-pyridone, a Watson–Crick mimic of adenine center dot uracil. *J Chem Phys* 121:8237–8245
10. Held A, Pratt DW (1992) Hydrogen bonding in the symmetry-equivalent C/sub 2h/ dimer of 2-pyridone in its S/sub 0/ and S/sub 2/ electronic states. Effect of deuterium substitution. *J Chem Phys* 96:4869–4876

11. Arrowsmith P, de Vries MS, Hunziker HE, Wendt HR (1988) Pulsed laser desorption near a jet orifice: concentration profiles of entrained perylene vapor. *Appl Phys B* 46:165–173
12. Meijer G, de Vries MS, Hunziker HE, Wendt HR (1990) Laser desorption jet-cooling of organic molecules. Cooling characteristics and detection sensitivity. *Appl Phys B* 51:395–403
13. Tembreull R, Lubman DM (1987) Resonant two-photon ionization of small peptides using pulsed laser desorption in supersonic beam mass spectrometry. *Anal Chem* 59:1003–1006
14. Weyssenhoff HV, Selzle HL, Schlag EW (1985) Laser-desorbed large molecules in a supersonic jet. *Zeitschrift für Naturforschung Teil A* 40a:674–676
15. Mayorkas N, Malka I, Bar I (2011) Ionization-loss stimulated Raman spectroscopy for conformational probing of flexible molecules. *PCCP* 13:6808–6815
16. Alonso JL, López JC (2014) Microwave spectroscopy of biomolecular building blocks. *Topcis Curr Chem*. doi:10.1007/128_2014_601
17. Lopez JC, Pena MI, Sanz ME, Alonso JL (2007) Probing thymine with laser ablation molecular beam Fourier transform microwave spectroscopy. *J Chem Phys* 2007:126
18. Vaquero V, Sanz ME, Lopez JC, Alonso JL (2007) The structure of uracil: a laser ablation rotational study. *J Phys Chem A* 111:3443–3445
19. Alonso JL, Pena I, Lopez JC, Vaquero V (2009) Rotational spectral signatures of four tautomers of guanine. *Angew Chem Int Ed* 48:6141–6143
20. Alonso JL, Vaquero V, Pena I, Lopez JC, Mata S, Caminati W (2013) All five forms of cytosine revealed in the gas phase. *Angew Chem Int Ed* 52:2331–2334
21. Lopez JC, Alonso JL, Pena I, Vaquero V (2010) Hydrogen bonding and structure of uracil-water and thymine-water complexes. *PCCP* 12:14128–14134
22. Merritt JM, Douberly GE, Miller RE (2004) Infrared-infrared-double resonance spectroscopy of cyanoacetylene in helium nanodroplets. *J Chem Phys* 121:1309–1316
23. Choi MY, Dong F, Miller RE (2005) Multiple tautomers of cytosine identified and characterized by infrared laser spectroscopy in helium nanodroplets: probing structure using vibrational transition moment angles. *Philos Trans R Soc Lond Ser A Mathemat Phys Eng Sci* 363:393–412
24. Smolarek S, Rijs AM, Buma WJ, Drabbls M (2010) Absorption spectroscopy of adenine, 9-methyladenine, and 2-aminopurine in helium nanodroplets. *PCCP* 12:15600–15606
25. Choi MY, Miller RE (2006) Four tautomers of isolated guanine from infrared laser spectroscopy in helium nanodroplets. *J Am Chem Soc* 128:7320–7328
26. Amirav A, Even U, Jortner J (1981) Absorption-spectroscopy of ultracold large molecules in planar supersonic expansions. *Chem Phys Lett* 83:1–4
27. Liu K, Fellers RS, Viant MR, McLaughlin RP, Brown MG, Saykally RJ (1996) A long path length pulsed slit valve appropriate for high temperature operation: infrared spectroscopy of jet-cooled large water clusters and nucleotide bases. *Rev Sci Instrum* 67:410–416
28. Viant MR, Fellers RS, McLaughlin RP, Saykally RJ (1995) Infrared-laser spectroscopy of uracil in a pulsed slit jet. *J Chem Phys* 103:9502–9505
29. Nir E, Janzen C, Imhof P, Kleinermanns K, de Vries MS (2001) Guanine tautomerism revealed by UV-UV and IR-UV hole burning spectroscopy. *J Chem Phys* 115:4604–4611
30. Nir E, Grace L, Brauer B, de Vries MS (1999) REMPI spectroscopy of jet-cooled guanine. *J Am Chem Soc* 121:4896–4897
31. Cerny J, Spirko V, Mons M, Hobza P, Nachtigallova D (2006) Theoretical study of the ground and excited states of 7-methyl guanine and 9-methyl guanine: comparison with experiment. *PCCP* 8:3059–3065
32. Chin W, Mons M, Piuzzi F, Tardivel B, Dimicoli I, Gorb L, Leszczynski J (2004) Gas phase rotamers of the nucleobase 9-methylguanine enol and its monohydrate: optical spectroscopy and quantum mechanical calculations. *J Phys Chem A* 108:8237–8243
33. Mons M, Dimicoli I, Piuzzi F, Tardivel B, Elhanine M (2002) Tautomerism of the DNA base guanine and its methylated derivatives as studied by gas-phase infrared and ultraviolet spectroscopy. *J Phys Chem A* 106:5088–5094

34. Chin W, Mons M, Dimicoli I, Piuze F, Tardivel B, Elhanine M (2002) Tautomer contribution's to the near UV spectrum of guanine: towards a refined picture for the spectroscopy of purine molecules. *Eur Phys J D* 20:347–355
35. Piuze F, Mons M, Dimicoli I, Tardivel B, Zhao Q (2001) Ultraviolet spectroscopy and tautomerism of the DNA base guanine and its hydrate formed in a supersonic jet. *Chem Phys* 270:205–214
36. Marian CM (2007) The guanine tautomer puzzle: quantum chemical investigation of ground and excited states. *J Phys Chem A* 111:1545–1553
37. Mons M, Piuze F, Dimicoli I, Gorb L, Leszczynski J (2006) Near-UV resonant two-photon ionization spectroscopy of gas phase guanine: evidence for the observation of three rare tautomers. *J Phys Chem A* 110:10921–10924
38. Seefeld K, Brause R, Häber T, Kleineremanns K (2007) Imino tautomers of gas-phase guanine from mid-infrared laser spectroscopy. *J Phys Chem A* 111:6217–6221
39. Asami H, Urashima S, Tsukamoto M, Motoda A, Hayakawa Y, Saigusa H (2012) Controlling glycosyl bond conformation of guanine nucleosides: stabilization of the anti conformer in 5'-O-ethylguanosine. *J Phys Chem Lett* 3:571–575
40. Asami H, Tsukamoto M, Hayakawa Y, Saigusa H (2010) Gas-phase isolation of diethyl guanosine 5'-monophosphate and its conformational assignment. *PCCP* 12:13918–13921
41. Abo-Riziq A, Crews BO, Compagnon I, Oomens J, Meijer G, Von Helden G, Kabelac M, Hobza P, de Vries MS (2007) The mid-IR spectra of 9-ethyl guanine, guanosine, and 2-deoxyguanosine. *J Phys Chem A* 111:7529–7536
42. Plützer C, Kleineremanns K (2002) Tautomers and electronic states of jet-cooled adenine investigated by double resonance spectroscopy. *PCCP* 4:4877–4882
43. Brown RD, Godfrey PD, McNaughton D, Pierlot A (1989) A study of the major gas-phase tautomer of adenine by microwave spectroscopy. *Chem Phys Lett* 156:61–63
44. Lee Y, Schmitt M, Kleineremanns K, Kim B (2006) Observation of ultraviolet rotational band contours of the DNA base adenine: determination of the transition moment. *J Phys Chem A* 110:11819–11823
45. Kim NJ, Jeong G, Kim YS, Sung J, Kim SK, Park YD (2000) Resonant two-photon ionization and laser induced fluorescence spectroscopy of jet-cooled adenine. *J Chem Phys* 113:10051–10055
46. Tomic K, Tatchen J, Marian CM (2005) Quantum chemical investigation of the electronic spectra of the keto, enol, and keto-imine tautomers of cytosine. *J Phys Chem A* 109:8410–8418
47. Trygubenko SA, Bogdan TV, Rueda M, Orozco M, Luque FJ, Sponer J, Slavicek P, Hobza P (2002) Correlated ab initio study of nucleic acid bases and their tautomers in the gas phase, in a microhydrated environment and in aqueous solution – Part 1. Cytosine *PCCP* 4:4192–4203
48. Kobayashi R (1998) A CCSD(T) study of the relative stabilities of cytosine tautomers. *J Phys Chem A* 102:10813–10817
49. Szczesniak M, Szczepaniak K, Kwiatkowski JS, Kubulat K, Person WB (1988) Matrix-isolation infrared studies of nucleic-acid constituents. 5. Experimental matrix-isolation and theoretical ab initio SCF molecular-orbital studies of the infrared-spectra of cytosine monomers. *J Am Chem Soc* 110:8319–8330
50. Brown RD, Godfrey PD, McNaughton D, Pierlot A (1989) Tautomers of cytosine by microwave spectroscopy. *J Am Chem Soc* 111:2308–2310
51. Trygubenko SA, Bogdan TV, Rueda M, Orozco M, Luque FJ, Sponer J, Slavicek P, Hobza P (2002) Correlated ab initio study of nucleic acid bases and their tautomers in the gas phase, in a microhydrated environment and in aqueous solution. Part 1. Cytosine. *PCCP* 4:4192–4204
52. Nir E, Muller M, Grace LI, de Vries MS (2002) REMPI spectroscopy of cytosine. *Chem Phys Lett* 355:59–64
53. Nir E, Hünig I, Kleineremanns K, de Vries MS (2003) The nucleobase cytosine and the cytosine dimer investigated by double resonance laser spectroscopy and ab initio calculations. *PCCP* 5:4780–4785

54. Nowak MJ, Szczepaniak K, Barski A, Shugar D (1978) Spectroscopic studies on vapor-phase tautomerism of natural bases found in nucleic-acids. *Z Naturforsch C* 33:876–883
55. Brown RD, Godfrey PD, McNaughton D, Pierlot A (1988) The microwave spectrum of uracil. *J Am Chem Soc* 110:2329–2330
56. Brown RD, Godfrey PD, McNaughton D, Pierlot AP (1989) Microwave-spectrum of the major gas-phase tautomer of thymine. *J Chem Soc Chem Comm* 1989:37–38
57. Kunitski M, Nosenko Y, Brutschy B (2011) On the nature of the long-lived “dark” state of isolated 1-methylthymine. *ChemPhysChem* 12:2024–2030
58. Oepts D, van der Meer AFG, van Amersfoort PW (1995) The free-electron-laser user facility FELIX. *Infrared Phys Technol* 36:297–308
59. van Zundert GCP, Jaqx S, Berden G, Bakker JM, Kleinermanns K, Oomens J, Rijs AM (2011) IR spectroscopy of isolated neutral and protonated adenine and 9-methyladenine. *ChemPhysChem* 12:1921–1927
60. Salpin JY, Guillaumont S, Tortajada J, MacAleese L, Lemaire J, Maitre P (2007) Infrared spectra of protonated uracil, thymine and cytosine. *ChemPhysChem* 8:2235–2244
61. Oomens J, Moehlig AR, Morton TH (2010) Infrared multiple photon dissociation (IRMPD) spectroscopy of the proton-bound dimer of 1-methylcytosine in the gas phase. *J Phys Chem Lett* 1:2891–2897
62. Yang B, Wu RR, Berden G, Oomens J, Rodgers MT (2013) Infrared multiple photon dissociation action spectroscopy of proton-bound dimers of cytosine and modified cytosines: effects of modifications on gas-phase conformations. *J Phys Chem B* 117:14191–14201
63. Ung HU, Moehlig AR, Kudla RA, Mueller LJ, Oomens J, Berden G, Morton TH (2013) Proton-bound dimers of 1-methylcytosine and its derivatives: vibrational and NMR spectroscopy. *PCCP* 15:19001–19012
64. Yang B, Wu RR, Polfer NC, Berden G, Oomens J, Rodgers MT (2013) IRMPD action spectroscopy of alkali metal cation-cytosine complexes: effects of alkali metal cation size on gas phase conformation. *J Am Soc Mass Spectrom* 24:1523–1533
65. Nei YW, Akinyemi TE, Kaczan CM, Steill JD, Berden G, Oomens J, Rodgers MT (2011) Infrared multiple photon dissociation action spectroscopy of sodiated uracil and thiouracils: effects of thioketo-substitution on gas-phase conformation. *Int J Mass spectrom* 308:191–202
66. Nei YW, Akinyemi TE, Steill JD, Oomens J, Rodgers MT (2010) Infrared multiple photon dissociation action spectroscopy of protonated uracil and thiouracils: effects of thioketo-substitution on gas-phase conformation. *Int J Mass spectrom* 297:139–151
67. Crampton KT, Rathur AI, Nei YW, Berden G, Oomens J, Rodgers MT (2012) Protonation preferentially stabilizes minor tautomers of the halouracils: IRMPD action spectroscopy and theoretical studies. *J Am Soc Mass Spectrom* 23:1469–1478
68. Nei YW, Crampton KT, Berden G, Oomens J, Rodgers MT (2013) Infrared multiple photon dissociation action spectroscopy of deprotonated RNA mononucleotides: gas-phase conformations and energetics. *J Phys Chem A* 117:10634–10649
69. Nei YW, Hallowita N, Steill JD, Oomens J, Rodgers MT (2013) Infrared multiple photon dissociation action spectroscopy of deprotonated DNA mononucleotides: gas-phase conformations and energetics. *J Phys Chem A* 117:1319–1335
70. Ligare M, Rijs AM, Berden G, Kabelac M, Nachtigallova D, Oomens J, de Vries MS (2014) Resonant IRMPD of nucleotide monophosphate anionic clusters. Submitted
71. Sobolewski AL, Domcke W, Hättig C (2005) Tautomeric selectivity of the excited-state lifetime of guanine/cytosine base pairs: the role of electron-driven proton-transfer processes. *Proc Natl Acad Sci U S A* 102:17903–17906
72. Nir E, Janzen C, Imhof P, Kleinermanns K, de Vries MS (2002) Pairing of the nucleobases guanine and cytosine in the gas phase studied by IR-UV double-resonance spectroscopy and ab initio calculations. *PCCP* 4:732–739
73. Mayorkas N, Izbitski S, Bernat A, Bar I (2012) Simultaneous ionization-detected stimulated raman and visible-visible-ultraviolet hole-burning spectra of two tryptamine conformers. *J Phys Chem Lett* 3:603–607

74. Brauer B, Gerber RB, Kabelac M, Hobza P, Bakker JM, Riziq AGA, de Vries MS (2005) Vibrational spectroscopy of the G center dot center dot center dot C base pair: experiment, harmonic and anharmonic calculations, and the nature of the anharmonic couplings. *J Phys Chem A* 109:6974–6984
75. Plützer C, Hünig I, Kleinermanns K, Nir E, de Vries MS (2003) Pairing of isolated nucleobases: double resonance laser spectroscopy of adenine-thymine. *ChemPhysChem* 4:838–842
76. Crews B, Abo-Riziq A, Grace L, Callahan M, Kabelac M, Hobza P, de Vries MS (2005) IR-UV double resonance spectroscopy of guanine-H₂O clusters. *PCCP* 7:3015–3020
77. Asami H, Yagi K, Ohba M, Urashima S, Saigusa H (2013) Stacked base-pair structures of adenine nucleosides stabilized by the formation of hydrogen-bonding network involving the two sugar groups. *Chem Phys* 419:84–89
78. Saigusa H, Urashima S, Asami H (2009) IR-UV double resonance spectroscopy of the hydrated clusters of guanosine and 9-methylguanine: evidence for hydration structures involving the sugar group. *J Phys Chem A* 113:3455–3462
79. Saigusa H, Urashima S, Asami H, Ohba M (2010) Microhydration of the guanine–guanine and guanine–cytosine base pairs. *J Phys Chem A* 114:11231–11237
80. Zeleny T, Hobza P, Kabelac M (2009) Microhydration of guanine center dot center dot center dot cytosine base pairs, a theoretical study on the role of water in stability, structure and tautomeric equilibrium. *PCCP* 11:3430–3435
81. Kabelac M, Ryjacek F, Hobza P (2000) Already two water molecules change planar H-bonded structures of the adenine . . . thymine base pair to the stacked ones: a molecular dynamics simulations study. *PCCP* 2:4906–4909
82. Callahan MP, Gengeliczki Z, Svadlenak N, Valdes H, Hobza P, de Vries MS (2008) Non-standard base pairing and stacked structures in methyl xanthine clusters. *PCCP* 10:2819–2826
83. Callahan MP, Crews B, Abo-Riziq A, Grace L, de Vries MS, Gengeliczki Z, Holmes TM, Hill GA (2007) IR-UV double resonance spectroscopy of xanthine. *PCCP* 9:4587–4591
84. Plützer C, Hünig I, Kleinermanns K (2003) Pairing of the nucleobase adenine studied by IR-UV double-resonance spectroscopy and ab initio calculations. *PCCP* 5:1158–1163
85. Smith VR, Samoylova E, Ritze HH, Radloff W, Schultz T (2010) Excimer states in microhydrated adenine clusters. *PCCP* 12:9632–9636
86. Malone RJ, Miller AM, Kohler B (2003) Singlet excited-state lifetimes of cytosine derivatives measured by femtosecond transient absorption. *Photochem Photobiol* 77:158–164
87. Nachtigallova D, Lischka H, Szymczak JJ, Barbatti M, Hobza P, Gengeliczki Z, Pino G, Callahan MP, de Vries MS (2010) The effect of C5 substitution on the photochemistry of uracil. *PCCP* 12:4924–4933
88. Mburu E, Matsika S (2008) An ab initio study of substituent effects on the excited states of purine derivatives. *J Phys Chem A* 112:12485–12491
89. Kistler KA, Matsika S (2007) Cytosine in context: a theoretical study of substituent effects on the excitation energies of 2-pyrimidinone derivatives. *J Phys Chem A* 111:8708–8716
90. Broo A (1998) A theoretical investigation of the physical reason for the very different luminescence properties of the two isomers adenine and 2-aminopurine. *J Phys Chem A* 102:526–531
91. Andreasson J, Holmén A, Albinsson B (1999) The photophysical properties of the adenine chromophore. *J Phys Chem B* 103:9782–9789
92. Mishra SK, Shukla MK, Mishra PC (2000) Electronic spectra of adenine and 2-aminopurine: an ab initio study of energy level diagrams of different tautomers in gas phase and aqueous solution. *Spectrochim Acta Part A* 56:1355–1384
93. Lührs DC, Viallon J, Fischer I (2001) Excited state spectroscopy and dynamics of isolated adenine and 9-methyladenine. *Phys Chem Chem Phys* 3:1827–1831
94. Kang H, Jung B, Kim SK (2003) Mechanism for ultrafast internal conversion of adenine. *J Chem Phys* 118:6717–6719

95. Sobolewski AL, Domcke W (2002) On the mechanism of nonradiative decay of DNA bases: ab initio and TDDFT results for the excited states of 9H-adenine. *Eur Phys J D* 20:369–374
96. Barbatti M, Lischka H (2007) Can the nonadiabatic photodynamics of aminopyrimidine be a model for the ultrafast deactivation of adenine? *J Phys Chem A* 111:2852–2858
97. Marian CM (2005) A new pathway for the rapid decay of electronically excited adenine. *J Chem Phys* 122:104314
98. Hünig I, Plützer C, Seefeld KA, Löwenich D, Nispel M, Kleinermanns K (2004) Photostability of isolated and paired nucleobases: N–H dissociation of adenine and hydrogen transfer in its base pairs examined by laser spectroscopy. *ChemPhysChem* 5:1427–1431
99. Crespo-Hernández CE, Cohen B, Hare PM, Kohler B (2004) Ultrafast excited-state dynamics in nucleic acids. *Chem Rev* 104:1977–2019
100. Zierhut M, Roth W, Fischer I (2004) Dynamics of H-atom loss in adenine. *PCCP* 6:5178–5183
101. Zechmann G, Barbatti M (2008) Ab initio study of the photochemistry of aminopyrimidine. *Int J Quantum Chem* 108:1266–1276
102. Kistler KA, Matsika S (2008) Three-state conical intersections in cytosine and pyrimidinone bases. *J Chem Phys* 128
103. Kistler KA, Matsika S (2007) Radiationless decay mechanism of cytosine: an ab initio study with comparisons to the fluorescent analogue 5-methyl-2-pyrimidinone. *J Phys Chem A* 111:2650–2661
104. Yarasi S, Brost P, Loppnow GR (2007) Initial excited-state structural dynamics of thymine are coincident with the expected photochemical dynamics. *J Phys Chem A* 111:5130–5135
105. Nir E, Kleinermanns K, de Vries MS (2000) Pairing of isolated nucleic-acid bases in the absence of the DNA backbone. *Nature* 408:949–951
106. Abo-Riziq A, Grace L, Nir E, Kabelac M, Hobza P, de Vries MS (2005) Photochemical selectivity in guanine-cytosine base-pair structures. *Proc Natl Acad Sci U S A* 102:20–23
107. Middleton CT, de La Harpe K, Su C, Law YK, Crespo-Hernandez CE, Kohler B (2009) DNA excited-state dynamics: from single bases to the double helix. *Annu Rev Phys Chem* 60:217–239